RESONANT OVER-REFLECTION AND TRANSMISSION OF ACOUSTIC WAVES IN COMPRESSIBLE SHEAR LAYERS

Simon Goertz, Lara De Broeck, Paul Hollmann and Martin Oberlack
Chair of Fluid Dynamics
Technische Universität Darmstadt
Otto-Berndt-Str. 2, 64287 Darmstadt, Germany
goertz@fdy.tu-darmstadt.de

ABSTRACT

We consider the reflection and transmission of acoustic waves by a compressible hyperbolic-tangent shear layer. The linearised Euler equations are solved by connecting singular Frobenius-series solutions about the two far-fields and about the critical layer. The analysis combines the causal selection of the logarithmic branch cut, a power-series construction of the scattering problem, and numerical results. For waves that are supersonic with respect to one far field, a resonant over-reflected mode is found, characterized by an infinite reflection coefficient. This resonant frequency is a neutral outgoing eigenmode and at the same time represents the neutral large-wavenumber limit of the linear instability modes. Further, waves that are supersonic with respect to both free streams, allow for both reflection and transmission and show finite over-reflection and over-transmission. Finally, equivalence transformations allow the considerations to be extended to three-dimensional and non-isothermal shear layers.

1 Introduction

Noise generation and propagation in compressible flows are of considerable practical relevance, since compressible and supersonic shear flows occur in many technical applications. For isothermal plane shear flows, the linearized Euler equations reduce, under a normal-mode ansatz, to the Pridmore–Brown equation (PBE) (Pridmore-Brown, 1958). The present work investigates fundamental mechanisms of acoustic-wave propagation, in particular reflection and transmission, and their relation to eigenmodes and instabilities.

In stability analysis, bounded or decaying far-field conditions imply attenuation of the solutions away from the shear layer. However, as radiating modes approach a purely oscillatory limit, their normal decay rate decreases together with the modal growth rate, so that the associated pressure fluctuations remain observable farther from the shear region. This motivates the existence of neutral waves with zero growth rate and finite-amplitude oscillatory behaviour in the far field. Such modes were first discussed by Groppengiesser (1969) and later analysed for the hyperbolic-tangent shear layer by Jackson & Grosch (1989), who identified two outgoing oscillatory neutral modes at supersonic Mach numbers. Their later observation that exact mode tracking requires detailed eigenfunction information provides one motivation for the present study (Jackson & Grosch, 1990).

Analytical solutions of the PBE are particularly useful for identifying the underlying wave propagation mechanisms. Following the asymptotic solutions of Pridmore-Brown (1958), such solutions have been developed for several velocity profiles. Even simple profiles may lead to special functions, such as parabolic-cylinder functions for linear profiles or confluent Heun functions for exponential boundary layers (Goldstein & Rice, 1973; Zhang & Oberlack, 2021). The singularities of the inviscid PBE determine the structure of its solutions. Of particular importance is the critical layer, where the streamwise phase velocity equals the local mean-flow velocity. There, logarithmic terms arise in the Frobenius expansions, and the associated jump in Reynolds stress is linked to instability mechanisms (Foote & Lin, 1950; Haberman, 1972). This makes the critical layer central to wave amplification during interaction with a shear layer.

A common approach is to consider an incident acoustic wave that is reflected and transmitted by the shear layer. If the reflected amplitude exceeds the incident one, the process is termed over-reflection. This mechanism was first discussed for acoustic waves at a vortex sheet by Miles (1957) and later related to energy transfer from the mean shear to the wave in geophysical contexts (Eltayeb & McKenzie, 1975). The connection between over-reflection and instability was subsequently investigated in several settings, including baroclinic, stratified and viscous shear flows (Lindzen *et al.*, 1980; Lindzen & Rosenthal, 1983; Lindzen & Rambaldi, 1986).

For acoustic waves governed by the PBE, Koutsoyannis *et al.* (1980) derived reflection and transmission coefficients for a piecewise-linear shear layer and found no acoustic resonance with respect to incident waves, indicating the importance of finite shear-layer thickness. More recently it was shown for supersonic boundary layers that over-reflection may also occur without a distinguished critical layer when viscous wall-layer effects dominate (Qin & Wu, 2016; Liu *et al.*, 2020). In the current work, causality arguments together with Frobenius-series solutions of the PBE are used to show that the critical layer is necessary for over-reflection and resonance in the hyperbolic tangent shear layer. Resonant over-reflection was already demonstrated by Qin & Wu (2024) for a BL, who showed that the resonant over-reflected mode coincides with a spontaneously emitted radiating mode.

PROBLEM FORMULATION

The analysis is based on an isothermal hyperbolic-tangent shear layer, which provides a suitable model for the mixing region of a coaxial jet-engine exhaust (Michalke, 1965). The velocity in the streamwise direction is given by

$$U_0(y) = \frac{1}{2}\left[1+\tanh(y)\right]. \tag{1}$$

The perturbations are represented by the normal-mode ansatz

$$q'(x,y,t) = \hat{q}(y)e^{i(\alpha x-\omega t)} \quad \text{with } q' \in (u',v',\rho',p',T'). \tag{2}$$

The compressible Rayleigh equation for the pressure amplitude reads

$$\hat{p}''(y) + \left(\frac{2\alpha U_0'(y)}{\omega-\alpha U_0(y)} + \frac{T_0'(y)}{T_0(y)}\right)\hat{p}'(y) + \left(\frac{M^2\left(\omega-\alpha U_0(y)\right)^2}{T_0(y)} - \alpha^2\right)\hat{p}(y) = 0. \tag{3}$$

For the isothermal case considered here, $T_0(y) = 1$, and (3) reduces to the PBE (Pridmore-Brown, 1958),

$$\hat{p}''(y) + \frac{2\alpha}{\omega-\alpha U_0(y)}\frac{dU_0}{dy}\hat{p}'(y) + \left[M^2(\omega-\alpha U_0(y))^2 - \alpha^2\right]\hat{p}(y) = 0. \tag{4}$$

Together with (1), the far-field solutions of (4) are

$$\hat{p}(y)|_{y\to-\infty} = A_1 e^{\sqrt{\theta_{-\infty}}y} + A_2 e^{-\sqrt{\theta_{-\infty}}y}, \tag{5a}$$

$$\hat{p}(y)|_{y\to\infty} = B_1 e^{-\sqrt{\theta_{\infty}}y} + B_2 e^{\sqrt{\theta_{\infty}}y}, \tag{5b}$$

where

$$\sqrt{\theta_{\pm\infty}} = \sqrt{-M^2(\omega-\alpha U_{\pm\infty})^2+\alpha^2}, \quad U_\infty = 1, \qquad U_{-\infty} = 0. \tag{6}$$

For neutral modes, $\alpha,\omega \in \mathbb{R}$, the sign of $\theta_{\pm\infty}$ determines whether a far-field branch is exponential or oscillatory. We distinguish upper-side oscillatory (USO), lower-side oscillatory (LSO), two-side oscillatory (TSO), and purely exponential (EXP) regimes. The corresponding parameter regions are shown in figure 1. In the remainder, $c_x = \omega/\alpha$ denotes the streamwise phase velocity.

We analyze the response of the flow to an incident wave. We define reflection and transmission coefficients as ratios between the amplitudes of the outgoing and incident far-field solution branches,

$$R = \frac{A_{\text{refl}}}{A_{\text{inco}}}, \qquad T = \frac{A_{\text{trans}}}{A_{\text{inco}}}. \tag{7}$$

The classification of a wave as incoming or outgoing is based on the far-field group velocity,

$$c_{g,y} = \pm\frac{k_y}{M^2\alpha\left(c_x-U_{\pm\infty}\right)}, \qquad k_y = \sqrt{M^2(\omega-\alpha U_{\pm\infty})^2-\alpha^2}. \tag{8}$$

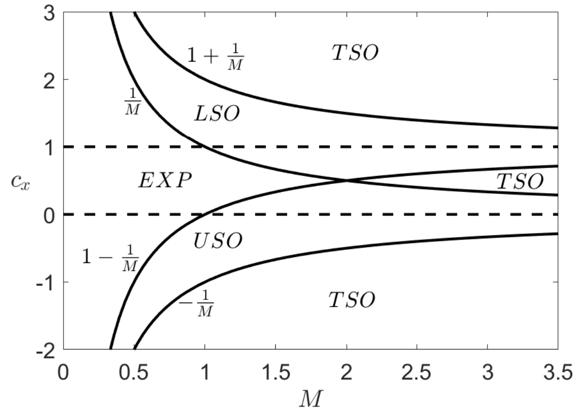

Figure 1: Neutral-mode regimes for $\omega,\alpha \in \mathbb{R}$: lower-side oscillatory solution (LSO), upper-side oscillatory solution (USO), two-side oscillatory solution (TSO), and purely exponential solution (EXP), depending on M and $c_x = \omega/\alpha$.

We may assume $\omega > 0$ w.l.o.g. With this assumption, the reflection and transmission coefficients are given by

$$R = \frac{A_2}{A_1}, B_2 = 0, \qquad \text{LSO}, \tag{9a}$$
$$R = \frac{B_1}{B_2}, A_2 = 0, \qquad \text{USO}, \tag{9b}$$
$$R = \frac{B_1}{B_2}, T = \frac{A_2}{B_2}, A_1 = 0, \qquad \text{TSO, incident from } \infty, \tag{9c}$$
$$R = \frac{A_2}{A_1}, T = \frac{B_1}{A_1}, B_2 = 0, \qquad \text{TSO, incident from } -\infty. \tag{9d}$$

FROBENIUS-SERIES CONNECTION

To facilitate a solution in terms of power series, the infinite physical interval is mapped to a finite interval by

$$z = U_0(y), \tag{10}$$

placing the singularities of the transformed PBE at $z_s = \{0, 1, c_x = \omega/\alpha, \infty\}$, where the far fields are mapped to 0 for $y \to -\infty$ and 1 for $y \to \infty$. A second transformation is applied to the dependent variable $\hat{p}$,

$$w(z) = z^{-\frac{1}{2}\sqrt{\theta_{-\infty}}} \cdot (1-z)^{-\frac{1}{2}\sqrt{\theta_{\infty}}} \cdot \hat{p}(z), \tag{11}$$

which brings the equation to a form equivalent to the general Heun equation. The Frobenius series expansions about the two far fields at $z = 0$ and $z = 1$ are

$$w(z,0) = A_1\sum_{n=0}^{\infty} a_{1,n}z^n + A_2\sum_{n=0}^{\infty} a_{2,n}z^{n-\sqrt{\theta_{-\infty}}}, \tag{12}$$

and

$$w(z,1) = B_1\sum_{n=0}^{\infty} b_{1,n}(1-z)^n + B_2\sum_{n=0}^{\infty} b_{2,n}(1-z)^{n-\sqrt{\theta_{\infty}}}. \tag{13}$$

The integration constants are exactly the same as in the far-field solutions (5a) and (5b) and can therefore be used directly to calculate reflection and transmission coefficients. If $c_x \in (0,1)$, a third local expansion is needed at the critical layer,

$$w(z,c_x) = D_1 \sum_{n=0}^{\infty} d_{1,n}\,(c_x - z)^{n+3} \tag{14}$$
$$+ D_2 \left(\sum_{n=0\setminus\{3\}}^{\infty} d_{2,n}\,(c_x - z)^n + d \sum_{n=0}^{\infty} d_{1,n}\,(c_x - z)^{n+3} \ln(c_x - z) \right),$$

where a causal branch cut must be chosen for the logarithmic terms, which will be explained below. Since the radii of convergence overlap on the real z-axis, the three series are connected at $z_0 \in (0, c_x)$ and $z_1 \in (c_x, 1)$ by

$$w(z_0, 0) = w(z_0, c_x), \tag{15}$$
$$w(z_1, 1) = w(z_1, c_x), \tag{16}$$
$$\left.\frac{\mathrm{d}w(z,0)}{\mathrm{d}z}\right|_{z=z_0} = \left.\frac{\mathrm{d}w(z,c_x)}{\mathrm{d}z}\right|_{z=z_0}, \tag{17}$$
$$\left.\frac{\mathrm{d}w(z,1)}{\mathrm{d}z}\right|_{z=z_1} = \left.\frac{\mathrm{d}w(z,c_x)}{\mathrm{d}z}\right|_{z=z_1}. \tag{18}$$

For a scattering problem, these conditions form a linear system for the unknown amplitudes once the incident wave has been prescribed. Dividing the connection equations by the amplitude of the incident wave gives

$$\mathbf{M} \cdot \left(R, T, \tilde{D}_1, \tilde{D}_2\right)^T = \mathbf{a}. \tag{19}$$

The matrix $\mathbf{M}$ contains the Frobenius branches representing the reflected and transmitted, or exponentially decaying, waves, together with the two critical-layer branches. The right-hand side $\mathbf{a}$ contains the values and derivatives of the unit-amplitude incident wave at the respective connection point. The constants $\tilde{D}_1$ and $\tilde{D}_2$ are the critical-layer integration constants scaled with the incident-wave amplitude.

This formulation is particularly convenient to find resonance frequencies. If the determinant of the outgoing-wave version of $\mathbf{M}$ vanishes, the homogeneous problem has a non-trivial solution without incident forcing. In the inhomogeneous scattering problem the same condition appears as a pole of R (or T). We call a pole in R resonant over-reflection.

CAUSALITY AT THE CRITICAL LAYER

The local solution (14) contains logarithms $\ln(c_x - z) = \ln|c_x - z| + i\arg(c_x - z)$. To uniquely define $\arg(c_x - z)$, a branch cut for the complex logarithm must be chosen. For a branch cut in the lower complex half plane, it holds for $z > c_x \in \mathbb{R}$ that $\arg(c_x - z) = \pi$. Vice versa, if the branch cut is chosen in the upper complex half plane, we obtain $\arg(c_x - z) = -\pi$. This branch cut cannot be chosen arbitrarily, instead the choice is made from a causality argument, which is briefly described in the following. For more details, the interested reader is referred to the work of Briggs (1964). The temporal response of the flow to any perturbation must vanish for $t < 0$. We recall that the normal mode approach (2) includes a Laplace transform in time. According to Briggs (1964), the inverse Laplace contour is placed in the complex ω-plane above all stability and neutral eigenvalues. To retain causality, it must be possible to close the inverse Laplace contour in the upper complex ω half plane with a semicircle at $|\omega| \to \infty$. This closed contour can only be drawn if no branch cut from the critical layer singularity emerges to the upper complex ω half plane. Accordingly, the logarithmic branch cut in (14) must be chosen in the lower complex half plane. Consequently, reflection and transmission coefficients are not merely determined by matching amplitudes; they also depend on the causal choice of the branch cut emerging from the critical layer.

In the following, we use the causal branch cut to show that $|R| > 1$ for waves with a critical layer, i.e. with $0 < c_x < 1$. We define

$$\bar{p}(y) = \frac{\hat{p}(y)}{c_x - U_0(y)}, \tag{20}$$

which transforms the PBE (4) to

$$\frac{\mathrm{d}^2 \bar{p}(y)}{\mathrm{d}y^2} + F(y)\bar{p}(y) = 0, \tag{21}$$

where $F(y)$ is real for neutral modes. We find that

$$I = \Im\left(\frac{\mathrm{d}\bar{p}}{\mathrm{d}y}\bar{p}^*\right) \tag{22}$$

is invariant above and below the critical layer. This follows because $\mathrm{d}I/\mathrm{d}y = 0$ above and below the critical layer. However, I may have a jump across it. We use the logarithmic series about the critical layer (14) to derive the leading order term of the jump of I across the critical layer as

$$[[I]] = I(y \to \infty) - I(y \to -\infty)$$
$$= -|C_2|^2 \cdot \frac{(2c_x - 1)\alpha^2 U_0'(y_c)}{4(1 - c_x)^3 c_x^3}\pi. \tag{23}$$

Since I is constant outside the critical layer, we can analogously use the asymptotic far field solutions to find an expression for the jump of I. This is done exemplary for USO solutions. For this particular case, we use (5b) to derive that

$$[[I]] = \frac{\sqrt{M^2(\omega - \alpha)^2 - \alpha^2}}{(c_x - 1)^2}\left(1 - |R|^2\right), \tag{24}$$

where $R = \frac{B_1}{B_2}$. Combining this result with (23) gives for USO waves $|R| > 1$. Analogously, the same conclusion can be drawn for LSO and TSO waves: If a critical layer is present, waves are always over-reflected. Note that this result is decisively influenced by a causal choice of the branch cuts. If a non-causal branch cut was chosen, the result would have been that the reflection coefficient is always smaller than one.

RESULTS

The numerical implementation evaluates the Frobenius series and their derivatives at the connection points z_0 and z_1, prescribes the incident far-field branch according to (9), and solves the resulting linear system for the outgoing amplitudes. The following presentation of the results separates two effects that are physically distinct: First, a resonant over-reflected mode is found in the USO and LSO regions, characterized by an infinite reflection coefficient. Second, we discuss finite reflection and transmission in the TSO region.

Resonant over-reflected modes

For waves that are oscillatory in only one far field, only the reflection coefficient is of interest, as defined in (9a) or (9b). We find a single point in the (c_x, α) plane where $|R|$ tends to infinity. This resonance is not characterized by a large but finite peak; it is a singular limit characterized by $\det \mathbf{M} = 0$ in (19). Therefore, a non-trivial solution exists without incident forcing. The resonant over-reflected frequency is thus a neutral outgoing eigenvalue of the shear layer.

This eigenvalue interpretation connects the scattering problem to the instability spectrum. We observe that the resonant over-reflected modes arise as continuations of unstable slow and fast instability modes and correspond to their neutral large-wavenumber limit. In the two-dimensional isothermal case, they occur as both USO/LSO solutions symmetric with respect to $c_x = 0.5$; both branches share the same wavenumber for a fixed Mach number. For the sake of brevity, the 2D results are not discussed here, instead, we directly turn to the consideration of 3D resonant over-reflected modes, which are generated from 2D results via the transformations

$$\alpha_{3\mathrm{D}} = \pm\Psi\,\alpha_{2\mathrm{D}}, \quad \omega_{3\mathrm{D}} = \pm\Psi\,\omega_{2\mathrm{D}}, \quad \beta = \pm\sqrt{1-\Psi^2}\,\alpha_{2\mathrm{D}}, \tag{25}$$

where β is the spanwise wavenumber and

$$\Psi = \frac{M_{2\mathrm{D}}}{M_{3\mathrm{D}}}, \tag{26}$$

defines a ratio between the respective Mach numbers for which 2D and 3D modes are calculated. These equivalence transformations map the differential equations and boundary conditions (BCs) formulated for the case of 2D propagating modes to their 3D equivalent and are analogous to the transformation found by Squire (1933) for the Orr-Sommerfeld and Squire equations. The results are presented in figures 2a,b, showing that the 3D resonance occupies a finite range of spanwise wavenumbers. The admissible β range grows with Mach number, and for sufficiently large Mach numbers multiple 3D modes may occur at the same spanwise wavenumber.

Quite analogously, equivalence transformations can be found for the special case of a non-isothermal shear layer. We introduce a simplification of the Crocco-Busemann (Crocco, 1932). For a shear layer with large temperature gradient, it may be valid that

$$T_0(y) = \tilde{T}_1(1-\tilde{T}_2\,U_0(y))^2, \tag{27}$$

with temperature ratio $\tilde{T}_1 = T_{-\infty}/T_\infty$ and $\tilde{T}_2 = 1-\sqrt{T_\infty/T_{-\infty}}$. This provides a reasonable simplification for $M \lesssim \sqrt{5}$. Details are omitted for brevity. However, for this temperature relation, we find an equivalence transformation between the CRE (3) and the PBE (4) as well as between the respective BCs as

$$\begin{aligned} \omega_T &= \pm\frac{\omega\alpha}{\alpha(1-\tilde{T}_2)+\omega\tilde{T}_2}, \\ \alpha_T &= \pm\alpha, \\ M_T &= \pm M\sqrt{\tilde{T}_1}\,\frac{\alpha(1-\tilde{T}_2)+\omega\tilde{T}_2}{\alpha}, \end{aligned} \tag{28}$$

where eigenvalues and Mach numbers referring to the non-isothermal case are indexed with a 'T'. These relations map the spectrum of non-isothermal resonant over-reflected modes to that of isothermal ones. The results are presented in figures 2c,d. We find that decreasing the temperature ratio, i.e. increasing the temperature gradient across the shear layer, shifts resonant over-reflected modes to lower Mach numbers. In addition, the isothermal symmetry about $c_x = 0.5$ is broken: the two far-field branches no longer share the same wavenumber and move apart as the temperature gradient increases. Note that for $\tilde{T}_1 < 0.025$, resonant over-reflected modes also occur for subsonic Mach numbers $M_T < 1$. Although the practical relevance of such extreme temperature ratios remains unclear, these results indicate that resonant over-reflection may occur in subsonic flows if the temperature gradient across the shear layer is sufficiently large.

Reflection and transmission in TSO

For TSO waves, both far fields are oscillatory and the incident wave produces one reflected and one transmitted outgoing branch. Owing to the reflection symmetry of the isothermal profile, it is sufficient to consider waves incident from the upper far field and a relation can be derived for the corresponding amplitude ratios for waves incident from the lower far field. This is left out here for the sake of brevity and we restrict the results to the case $M = 3$.

Figure 3 shows the reflection and transmission coefficients for a critical layer as a function of the streamwise phase velocity. The dominant feature is the presence of local maxima in both $|R|$ and $|T|$, corresponding to finite over-reflection and over-transmission. The maxima of the two coefficients do not generally occur at exactly the same phase velocity, indicating that the critical layer acts differently on reflected and transmitted waves. Increasing the frequency weakens the local maxima and the reflection coefficient approaches the total-reflection behaviour, which was found at the neighbouring one-side oscillatory boundaries.

We further analyze the TSO case in the absence of a critical layer. It provides a useful benchmark for the numerical method. If no critical layer is present, the jump of the invariant (22) vanishes and, for waves incident from the upper free stream, it can be derived that

$$\frac{\sqrt{-\theta_\infty}}{(c_x-1)^2}\left(1-|R|^2\right) - \frac{\sqrt{-\theta_{-\infty}}}{{c_x}^2}|T|^2 = 0. \tag{29}$$

This relation implies $|R| < 1$ for non-critical TSO waves, while both $|T| \lesseqgtr 1$ remain possible. The numerical results in figure 4 confirm this behaviour for $c_x > 1 + 1/M$: the reflection coefficient remains below unity, approaches $|R| \to 1$ near the adjacent one-side oscillatory region, and decreases for increasing phase velocity. By contrast, over-transmission occurs even without a critical layer. $|T| \to 1$ is approached for sufficiently large phase velocities. The results shown in the figure match the theoretical prediction from equation (29) up to machine precision.

CONCLUSIONS

A Frobenius-series connection method has been used to compute acoustic reflection and transmission in a compressible hyperbolic-tangent shear layer. The essential theoretical step is the causal selection of the logarithmic branch cut at the critical layer. This selection fixes the jump of an invariant across the critical layer and implies over-reflection for waves that possess a critical layer.

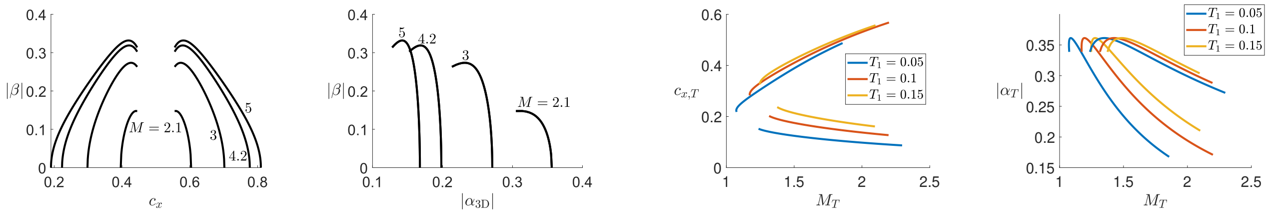

(a) (b) (c) (d)

Figure 2: Resonant over-reflected eigenmodes beyond the 2D isothermal base case. Panels (a) and (b) show 3D modes: spanwise wavenumber $|\beta|$ versus streamwise phase velocity c_x and streamwise wavenumber $|\alpha_{3\mathrm{D}}|$. Panels (c) and (d) show non-isothermal 2D modes: streamwise phase velocity $c_{x,T}$ and streamwise wavenumber $|\alpha_T|$ versus Mach number for several temperature ratios $\tilde{T}_1$.

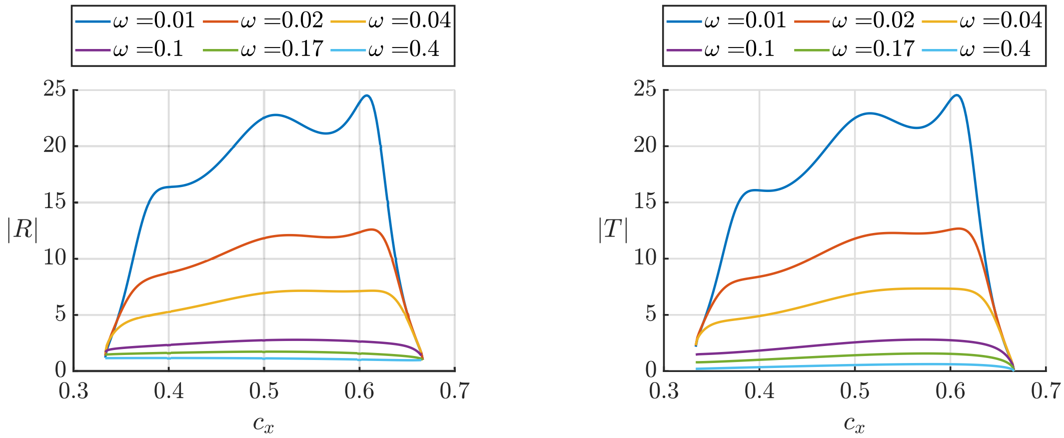

(a) (b)

Figure 3: Absolute values of the reflection and transmission coefficient for critical TSO modes at $M = 3$ under varying frequency: (a) reflection coefficient and (b) transmission coefficient.

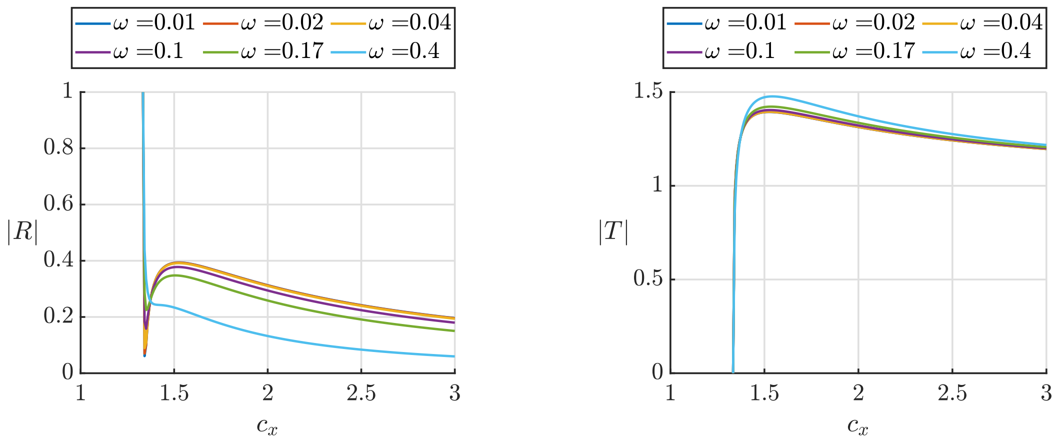

(a) (b)

Figure 4: Absolute values of the reflection and transmission coefficient for non-critical TSO modes with $c_x > 1 + 1/M$ at $M = 3$ under varying frequency: (a) reflection coefficient and (b) transmission coefficient.

We observe an acoustic resonance phenomenon with reflection coefficient $R \to \infty$. This resonance frequency is a neutral outgoing eigenmode and connects the scattering problem to the instability spectrum. From the 2D propagating solutions, we generate families of three-dimensional and non-isothermal resonant over-reflected modes through equivalence transformation, showing that a temperature gradient across the shear layer allows for the occurrence of resonant over-reflected modes even at subsonic Mach numbers. Further, results are presented for reflection and transmission coefficients for waves which are oscillatory in both far fields. There, we observe that a critical layer is necessary and sufficient for over-reflection. In contrast, transmitted waves are either amplified or attenuated, depending on their streamwise phase velocity. Over-transmission is possible for both solutions with or without a critical layer.

ACKNOWLEDGEMENTS

S. Görtz and M. Oberlack acknowledge funding by the Deutsche Forschungsgemeinschaft (DFG, German Research Foundation) – SPP 2410 Hyperbolic Balance Laws in Fluid Mechanics: Complexity, Scales, Randomness (CoScaRa), within the Project "Approximation Methods for Statistical Conservation Laws of Hyperbolically Dominated Flow" under project number 526024901. L. De Broeck acknowledges funding by the Deutsche Forschungsgemeinschaft (DFG, German Research Foundation) – OB 96/55-1 – 456793479. The work of S. Görtz, L. De Broeck and P. Hollmann was further supported by the Graduate School CE within the Centre for Computational Engineering at Technische Universität Darmstadt.

REFERENCES

Briggs, R. J. 1964 *Electron-Stream Interaction with Plasmas*. The MIT Press.

Crocco, L. 1932 Transmission of heat from a flat plate to a fluid flowing at a high velocity. *National Advisory Committee for Aeronautics* **NACA-TM-690**.

Eltayeb, I. A. & McKenzie, J. F. 1975 Critical-level behaviour and wave amplification of a gravity wave incident upon a shear layer. *J. Fluid Mech.* **72** (4), 661–671.

Foote, J. R. & Lin, C. C. 1950 Some recent investigations in the theory of hydrodynamic stability. *Quart. Appl. Math.* **8** (3), 265–280.

Goldstein, M. & Rice, E. 1973 Effect of shear on duct wall impedance. *J. Sound Vib.* **30** (1), 79–84.

Groppengiesser, H. 1969 Inviscid spatial stability of a compressible mixing layer. *NASA Tech. Translation* **F-12786**.

Haberman, R. 1972 Critical layers in parallel flows. *Stud. Appl. Math.* **51** (2), 139–161.

Jackson, T. L. & Grosch, C. E. 1989 Inviscid spatial stability of a compressible mixing layer. *J. Fluid Mech.* **208**, 609–637.

Jackson, T. L. & Grosch, C. E. 1990 On the classification of unstable modes in bounded compressible mixing layers. In *Instability and Transition* (ed. M. Y. Hussaini & R. G. Voigt), pp. 187–198. New York, NY: Springer New York.

Koutsoyannis, S. P., Karamcheti, K. & Galant, D. C. 1980 Acoustic resonances and sound scattering by a shear layer. *AIAA J.* **18** (12), 1446–1454.

Lindzen, R. S., Farrell, B. & Tung, K. 1980 The Concept of Wave Overreflection and Its Application to Baroclinic Instability. *J. Atmos. Sci.* **37** (1), 44–63.

Lindzen, R. S. & Rambaldi, S. 1986 A study of over-reflection in viscous poiseuille flow. *J. Fluid Mech.* **165**, 355–372.

Lindzen, R. S. & Rosenthal, A. J. 1983 Instabilities in a Stratified Fluid Having One Critical Level. Part III: Kelvin-Helmholtz Instabilities as Overreflected Waves. *J. Atmos. Sci.* **40** (3), 530–542.

Liu, Y., Dong, M. & Wu, X. 2020 Generation of first Mack modes in supersonic boundary layers by slow acoustic waves interacting with streamwise isolated wall roughness. *J. Fluid Mech.* **888**, A10.

Michalke, A. 1965 On spatially growing disturbances in an inviscid shear layer. *J. Fluid Mech.* **23** (3), 521–544.

Miles, J. W. 1957 On the generation of surface waves by shear flows. *J. Fluid Mech.* **3** (2), 185–204.

Pridmore-Brown, D. C. 1958 Sound propagation in a fluid flowing through an attenuating duct. *J. Fluid Mech.* **4** (4), 393—-406.

Qin, F. & Wu, X. 2016 Response and receptivity of the hypersonic boundary layer past a wedge to free-stream acoustic, vortical and entropy disturbances. *J. Fluid Mech.* **797**, 874–915.

Qin, F. & Wu, X. 2024 Excitation and evolution of radiating modes in supersonic boundary layers. part 1. fundamental resonance with impinging sound waves. *J. Fluid Mech.* **985**, A13.

Squire, H. B. 1933 On the stability for three-dimensional disturbances of viscous fluid flow between parallel walls. *Proc. R. soc. Lond. Ser. A-Contain. Pap. Math. Phys. Character* **142** (847), 621–628.

Zhang, Y. & Oberlack, M. 2021 Inviscid instability of compressible exponential boundary layer flows. *AIP Adv.* **11** (10), 105308.